Applied Chemical Engineering (2025) Volume 8 Issue 1 ISSN: 2578-2010 (O)
doi: 10.59429/ace.v8i1.5645

RESEARCH ARTICLE

Influence of the experimental setup parameters on the deviation of the similarity criteria in the experimental study of the model boundary conditions from the similarity criteria of the full-scale combustion chamber

S.K. Osipov, P.A. Bryzgunov, M.M Shaikh*, D.S. Pisarev, A.N. Vegera

Department of Innovative Technologies for High-Tech Industries, National Research University "Moscow Power Engineering Institute", Moscow, 111250, Russia

***Corresponding author:** Muhammad Maaz Shaikh, maazshaikh_2015@outlook.com.

ABSTRACT

This study investigates the combustion processes of methane in an oxygen and carbon dioxide environment within oxygen-fuel energy complexes (OFC). The unique operating conditions, characterized by high pressures (up to 300 atm) and the use of CO2 as a diluent, necessitate a thorough understanding of the combustion dynamics, which differ significantly from traditional gas turbine units (GTU). An experimental setup, inspired by existing literature, is proposed to evaluate the combustion characteristics of methane under these conditions.

Key objectives include establishing similarity criteria for hydrodynamic, thermal, and mass transfer processes to ensure the validity of experimental results. The analysis identifies critical parameters such as Reynolds, Euler, Boltzmann, Prandtl, and Damköhler numbers, which serve as benchmarks for achieving operational similarity between model and natural combustion scenarios. The findings indicate that while complete similarity across all criteria is unattainable, satisfactory levels can be achieved for specific processes under controlled conditions.

The proposed experimental stand is designed to replicate the conditions of OFC combustion chambers, incorporating advanced measurement systems for accurate monitoring of temperature, pressure, and flow rates. The study emphasizes the importance of conducting separate tests for mass transfer processes to ensure comprehensive evaluations of combustion dynamics.

This research provides valuable insights for the design and optimization of burner devices in OFC applications, contributing to the advancement of cleaner and more efficient energy production technologies. The established methodologies and criteria can guide future experimental studies, enhancing the understanding of combustion processes in high-pressure environments.

Keywords: combustion chamber; SCO2; GTU; similarity criteria

ARTICLE INFO

Received: 28 March 2025
Accepted: 17 April 2025
Available online: 29 April 2025

1. Introduction

Changes in the component composition and thermodynamic parameters of the working environment relative to traditional GTU operating conditions predetermine changes in the nature of the combustion process. In the combustion chamber (CC) of the oxygen-fuel energy complex (OFC), combustion of natural gas with oxygen occurs in a CO_2 diluent environment at a pressure of about 300 atm, which greatly differs the operating conditions from classic GTU combustion chambers, where air is the diluent. The specifics of the organization of mixing and combustion processes create the need for an experimental study of the methane combustion process in an O_2 and CO_2 environment. In the publication[1], Toshiba demonstrated a setup for testing the combustion chamber of an OFC operating on the Allam cycle, with a capacity of 5 MW at a pressure of 300 atm. Stable flame behavior was observed. At present, Russia has no experimental base for testing burner devices of OFC combustion chambers. The creation of an experimental stand that allows testing burner devices at supercritical parameters and capacities of more than 1 MW requires large financial costs and imposes increased safety requirements. Cost reduction is achieved by conducting tests under conditions different from natural ones, in which the pressure of the working fluid is lower and similarity of the processes of gas dynamics and heat and mass transfer processes is ensured. The described similarity of conditions is possible if the similarity criteria are met[2].

The research discusses the characteristics of combustion in direct-flow swirling combustors, emphasizing the need for physical and mathematical models based on empirical data and theoretical hypotheses. It notes that while the vortex interaction hypothesis effectively describes certain phenomena, the understanding of combustion mechanisms in swirling flows is still limited, with few reliable analytical methods available for calculating burner performance. The authors propose developing a system of similarity criteria using dimensionless forms of the Navier-Stokes equations, which will include various similarity numbers such as Euler, Schmidt, Froude, Reynolds, Mach, and Prandtl. This approach aligns with our research paper, which also explores similarity criteria to enhance the understanding of aero-thermochemical processes in combustion systems[3].

Much attention is paid to the selection of the similarity criteria base for physical-chemical and gas-dynamic processes in the publication[4]. The application of similarity criteria to laminar-diffusion combustion was considered, since the mixing of components is a characteristic of turbulent processes. Exchange-kinetic criteria characterize the share of heat exchange by all types of heat transfer from the heat of a chemical reaction, which are reduced to the Peclet, Boltzmann, and Nusselt heat exchange criteria. Heat exchange criteria can be replaced by the efficiency of the installation, which takes into account heat loss to the environment.

An oxygen-fuel cycle that differs from the Allam cycle in the composition of the working medium, but uses recycled CO2, was studied by the authors of the clean study Energy Systems (CES)[5] when considering the 16.4 bar superheater of the 170 MW OFT -900 combustor.

The process research is being conducted by a private consortium, which limits access to detailed combustion characteristics, but the main characteristics of the setup shown in **Figure 1** are known:

1) the superheater power varied from 4.3 to 5.4 MW, the CO2 concentration - from 41 to 44% vol., the pressure - from 9.5 to 10 bar, the operating time - from 11 to 65 minutes;
2) the working environment consists of 85-90% water vapor and 10-15% CO2. The use of such a mixture increased the heat capacity of combustion products by 60% and reduced the molecular weight of the environment, which led to a 20% increase in power during modernization;
3) water is injected into the flue gases to cool them to 316°C and then the gases are heated in a superheater to 1080°C;
4) In the superheater, pressure losses were 2.5-3%, the temperature distribution coefficient was 0.1.

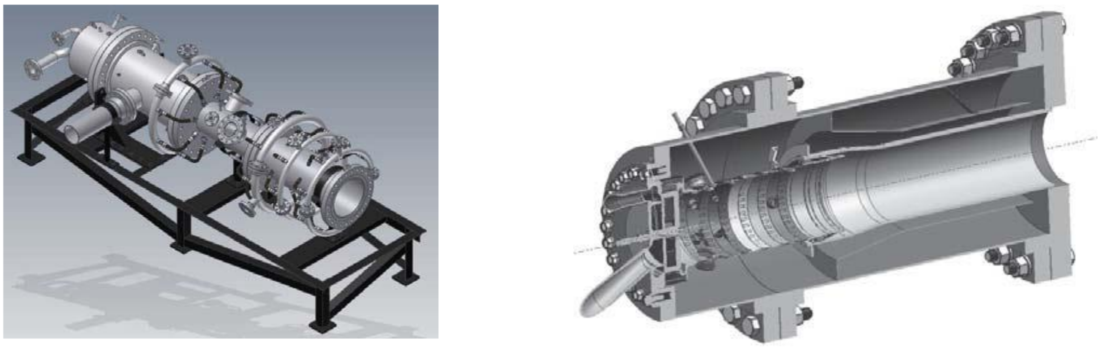

(A)

(b)

Figure 1 Solid models of the OFT -900 superheater test bench: (a) – test bench, (b) – cutout of the middle part of the combustion chamber sections.

In a publication devoted to the study of oxygen-fuel combustion in a CO2 environment[6], a diagram of the stand is given in **Figure 2** and its design is shown in **Figure 3**.

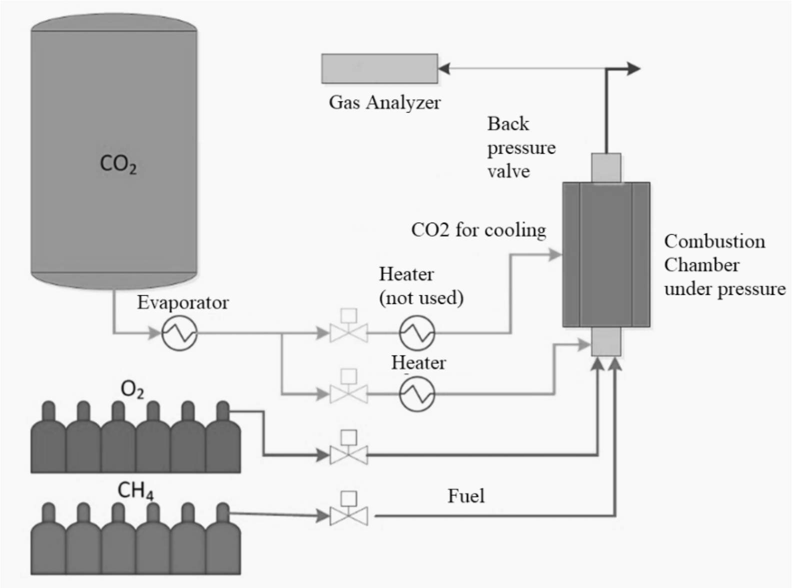

Figure 2 Experimental stand diagram[6].

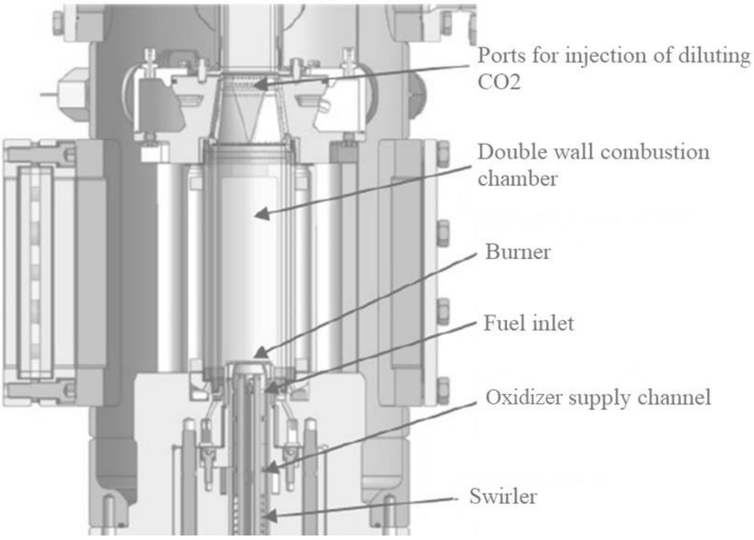

Figure 3. 3Stand for combustion of methane in CO2 environment[6].

The tests were carried out at a pressure of 1 to 10 bar for burner capacities of 10 to 100 kW. The concentration levels of CO and O_2 were measured at the outlet after the mixing zone chamber. The cooling flow of CO_2 was supplied between the quartz walls to the mixing zone. The outlet section of the burner device is 20 mm, the combustion chamber of cylindrical cross-section has a diameter of 50 mm and a length of 200 mm and is made of quartz. Methane was mixed with the oxidizer before the outlet of the burner. The vortex flow formed in the oxidizer channel stabilized the flame both at the immediate outlet of the burner and at a distance from it. In the stabilization modes at the outlet of the burner, the flame stability is higher, but there is a probability of breakthrough and overheating of the burner in the V -shaped flame mode. The M-shaped flame shape with combustion in the outer recirculation zones is safer from the burner integrity point of view and was observed in modes between the V -shaped attached and raised flame shapes.

The flame stabilization limit for oxygen concentration was determined to be 31.7% for a range of capacities from 10 to 40 kW. Exceeding the concentration directed the flame into the burner. With increasing pressure, the residence time in the chamber increases by 5 times, but this does not lead to a reduction in CO emissions.

In[7], the authors describe an experimental setup for burning hydrogen at a pressure of 15 MPa in a 980 mm long flame tube with an internal diameter of 27 mm.

Thus, based on the results of the literature analysis, requirements for the structure of the stand and its measurement system were established. In particular, the stand must provide for measurement of:

1) consumption of fuel, oxidizer and diluent;

2) temperatures and pressures of fuel, oxidizer and diluent at the entrance to the combustion chamber;

3) characteristic temperatures in the combustion zone;

4) temperature and composition of gases at the outlet of the experimental section.

In this case, due to the high temperatures of the torch, the working section of the stand must have sufficient thermal insulation made of non-combustible material. To measure temperatures and concentrations of gases at the exit from the working section, a turn of the gas duct must be provided in order to create a shadow zone and minimize the effect of torch radiation on the readings of the temperature sensors.

A separate issue in the physical modeling of combustion processes is the possibility of using the obtained data in the analysis of burner devices of higher power. The paper[8] presents a review of experimental studies of burner devices, as well as an analysis of the applicability of the results of studying small-scale laboratory burner devices to the analysis of industrial-capacity devices. The authors of the article conclude that absolute applicability is possible only if all similarity criteria are met, but when moving from a laboratory scale to an industrial one, the fuel and oxidizer consumption inevitably increases, which leads to an increase in the convective component in heat and mass transfer processes, which leads to the fact that the physics of the processes changes significantly, and sensitivity to small changes in the boundary conditions at the input and output disappears. However, the value of these studies is also high, since it allows determining qualitative dependencies.

Conducting experimental studies of small-scale burner devices is also relevant when studying large-scale industrial devices, as it allows obtaining experimental data that can be used to calibrate mathematical models used later when calculating a full-scale chamber. This approach is considered in the work[9], where experimental data for a small furnace were used to adjust combustion models when calculating an industrial-scale furnace. The deviation of the modeling data from natural conditions for heat flows was 1.9%, which is a good accuracy for engineering calculations.

Thus, based on the results of the analysis of the applicability of laboratory studies, the following conclusions can be drawn:

1) for the unconditional use of experimental data in the design of an industrial burner device, complete coincidence is required for all similarity criteria;
2) on a laboratory scale it is impossible to achieve similarity between heat and mass transfer processes and natural industrial burner devices;
3) Experimental data obtained from the study of small-scale burner devices can be successfully used to adjust combustion models used in the calculation of full-scale ones.

2. Methodology

Table 1 shows all the equipment used for experimental setup.

Table 1. List of components and services required for stand modernization.

Device/accessory	Name
CO2 flow meter	EE741-A6D2AC2DN15
Flow meter for O_2	EE741-A6D2AC2DN15
Flow meter for CH_4	Gas flow meter (Rotameter) MFM-50 with manual valve
Absolute pressure sensor	PD100I-DA2.5-111-0.25
High temperature thermocouples	DTPs thermocouples " platinum -rhodium-platinum" 20 cm length
Conventional thermocouples	DTPHhhh5 wire thermocouples with switching head

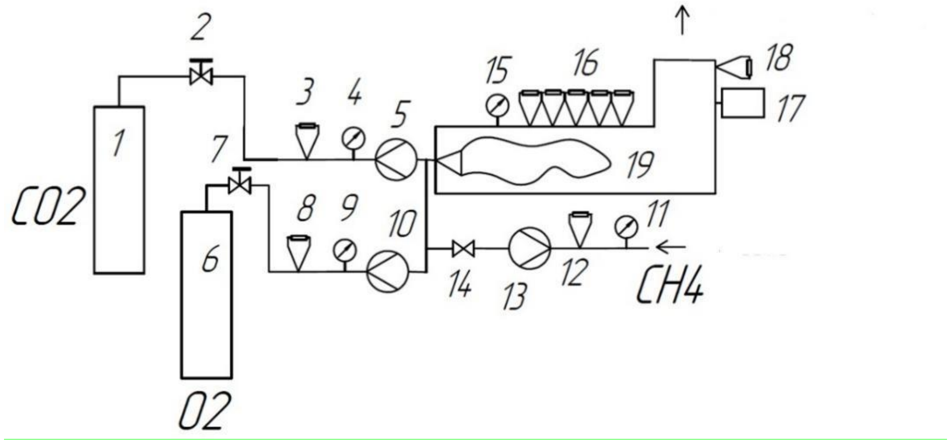

Figure 4. Scheme of the stand after modernization.

Natural gas enters the burner device from the network, while the gas flow is regulated by the valve (14) and measured by the flow meter (13). The temperature and pressure of the natural gas are measured by the thermocouple (12) and the pressure sensor (11), respectively. In the burner device, the fuel, oxidizer and diluent are mixed, and the fuel is burned in the working section (19). The pressure and temperature in the combustion zone are measured by the pressure sensor (15) and the temperature sensors (16), respectively. The temperature of the combustion products at the outlet is measured by the temperature sensor (18), the composition of the gases is measured by a gas analyzer or chromatograph, the measurement is carried out in the selection (17).

To detect the concentration of unburned methane, a chromatograph with a PID detector is used. PID is a sample-destructive, selective, flow detector. The linear range is over 107. The PID operates based on the change in the background current of a hydrogen flame when an organic substance is introduced into it. Organic substances, burning in a hydrogen flame, cause a current to flow between the collector electrode and the detector burner, to which voltage is applied. The current flowing is proportional to the amount of organic substance burned in the detector flame. The PID detects most organic compounds containing a C–H bond. The detector is sensitive to almost all organic compounds (not sensitive to formaldehyde and formic acid).

To detect the concentration of inert gases, a portable gas analyzer MRU is used. Optima 7. This device will be used to determine the concentrations of carbon dioxide, oxygen, carbon monoxide.

Since the oxidizer and diluent are supplied from cylinders in the proposed scheme, it is necessary to estimate the number of cylinders required to conduct the experiment, provided that the required power is maintained. In order to ensure a reserve in terms of the experiment time, the number of cylinders is calculated at the maximum thermal power of the stand. The mass flow rates of oxygen and carbon dioxide were determined based on the condition of maintaining the stoichiometric ratio for combustion of natural gas, with the oxidizer excess factor set at 1.05. The component flow rates at the maximum possible thermal power are summarized in **Table 2**.

Table 2. Component consumption and experiment times for a combustion chamber with a thermal power of 15 kW.

Parameter	**Methane CH4**	**Oxygen O2**	**Carbon dioxide CO2**
Mass flow rate, G, kg/s	0,0004	0,0015	0.0069
Volumetric flow rate, V, l/s	0.428	0,890	2,929
Volumetric flow rate, V, m3 $^{/}$ s	0,00043	0,001	0.003
Volume flow, V, m ^{3} / h	1,540	3,203	10,546
Maximum weight of gas cylinder, kg	22.5	8.3	19
Operating time of one cylinder, min.	1036	91	46

Thus, in the process of conducting future experimental research on the created stand, a burner device designed for the nominal power of the experimental stand - 15 kW will be tested. Since at this power it is impossible to ensure an acceptable deviation for all similarity criteria, then during the experiment the power of the burner device will also change by reducing the flow rate of the supplied natural gas.

The system of differential equations describing gas-dynamic processes and heat and mass transfer processes in a chemically reacting flow, which is a homogenous mixture, during combustion of gaseous fuel at low Mach numbers (the approximation of an ideal incompressible gas) consists of a system of equations that includes the laws of conservation of mass (1), momentum (2), thermal energy (3) and transport of impurities (4) [10]:

$$\frac{\partial(\rho v_i)}{\partial x_i} = 0 \tag{1}$$

$$\frac{\partial}{\partial x_j}(\rho v_i v_j) = -\frac{\partial p}{\partial x_i} + \frac{\partial}{\partial x_j}\left(\mu \frac{\partial v_i}{\partial x_j}\right) + \rho g_i \tag{2}$$

$$\frac{\partial}{\partial x_j} \cdot \left(c_p \rho v_j T\right) = \frac{\partial}{\partial x_j}\left(\lambda \frac{\partial T}{\partial x_j}\right) + q_{chem} + q_{rad} \tag{3}$$

$$\frac{\partial}{\partial x_j} \cdot \left(\rho_v v_j r_v\right) = \rho \frac{\partial}{\partial x_j}\left(D \frac{\partial r_v}{\partial x_j}\right) + S_{chem} \tag{4}$$

where ρis the density, kg/m3;

v – current velocity, m/s;

x – coordinate, m;

c_p– specific heat capacity, J/(kg ·K);

λ– thermal conductivity, W/(m·K);

μ– dynamic viscosity, Pa · s;

r – mass concentration;

p – pressure, Pa;

T – temperature, K;

g – acceleration of gravity, m/s^2 .

In equations (1-3), scalar quantities without indices refer to the mixture as a whole, and the index *v* indicates belonging to *the v* -th phase of the mixture, while the indices i,j refer to the coordinate system and the corresponding projections of the flow velocity vector of the homogeneous mixture, while the density and other thermophysical properties are a function of temperature. Due to the low flow velocities in the combustion chambers under consideration, the effects of gas compressibility may not be taken into account. The flow is also considered stationary and steady, due to which the changes in quantities over time are not taken into account in relations (1-4).

In equation (2), the term $\rho v_j \frac{\partial v_i}{\partial x_j}$is associated with the convective transfer of momentum, $\frac{\partial}{\partial x_j}\left(\mu \frac{\partial v_i}{\partial x_j}\right)$is associated with the viscous transfer of momentum, and $-\frac{\partial p}{\partial x_i}$determines the influence of the pressure difference, and $\rho g_i$is associated with the force of gravity.

In equation (3), the term $\frac{\partial}{\partial x_j} \cdot \left(c_p \rho v_j T\right)$is responsible for the convective transfer of energy, $\frac{\partial}{\partial x_j}\left(\lambda \frac{\partial T}{\partial x_j}\right)$is responsible for the conductive transfer of energy due to thermal conductivity, $q_{chem}$is responsible for the sources of heat release during chemical reactions, and $q_{rad}$is responsible for heat exchange by radiation.

Equation (4) is constructed similarly: the term $\frac{\partial}{\partial x_j} \cdot \left(\rho_v v_j r_v\right)$is associated with the convective transfer of impurity, $\frac{\partial}{\partial x_j}\left(D \frac{\partial r_v}{\partial x_j}\right)$with the transfer of impurity due to diffusion, and $S_{chem}$with the sources of impurity due to chemical reactions.

Analysis of the system of equations (2-4) allows us to draw a conclusion about the similarity of the equations describing physical processes, which allows us to apply the theory of similarity to analyze these processes. When a liquid flows, the conditions determining the similarity of the processes are the relationships between the main terms of the equation of conservation of momentum (2), namely[11]:

1) the ratio of convective momentum transfer to the transfer due to viscous friction forces;
2) the ratio of the force factors of the pressure gradient to the convective transfer of momentum;
3) the ratio of the force factors of gravity to the convective transfer of momentum.

Due to the connection of each relationship with the convective impulse, the equality of the above relationships for the model conditions of the experiment and the natural conditions of the real process will ensure the equality of the relationships of all members determining the forces acting on the volume of liquid between themselves, which in turn will allow us to judge the presence of hydrodynamic similarity. Thus, from the point of view of hydrodynamic similarity, the determining criteria will be[12]:

1) Reynolds number;
2) Euler's number;
3) Froude number.

When analyzing the energy conservation equation (3), we can conclude that the determining factors will be:

1) the ratio of convective energy transfer to conductive energy transfer due to thermal conductivity;
2) the ratio of convective energy transfer to transfer due to radiative heat exchange;
3) the ratio of convective energy transfer to the thermal effect of chemical reactions.

In this case, the similarity criteria are also related to the convective energy transfer, which, if they coincide, will provide the necessary relationships between the terms. Thus, for heat exchange, the determining similarity numbers will be[13]:

1) Peclet's number;
2) Boltzmann number;
3) Damköhler number.

Similarly, for the equation of impurity transport the determining factors will be:

1) the ratio of convective transport of impurities to molecular transport due to diffusion;
2) the ratio of convective mass transfer to transfer due to chemical reactions.

The determining similarity criteria for the impurity transport equation will be [14]:

1) Sherwood number;
2) Damköhler number .

It is important to note that the Peclet number and the Sherwood number are related to the Reynolds number through the following relationships:

$$Pe = Re \cdot Pr \tag{5}$$

$$Sh = f(Re, Sc) \tag{6}$$

where Re is the Reynolds number;

Pe – Peclet number;

Pr – Prandtl number;

Sh – Sherwood number;

Sc – Schmidt number.

From (5, 6) it follows that the Sherwood and Peclet numbers can be excluded from the system of similarity criteria, replacing them with the Schmidt and Prandtl numbers, respectively. In addition, due to the smallness of gravity forces in comparison with inertial forces, the Froude number can also be excluded.

Thus, there is a set of criteria, the fulfillment of which ensures complete similarity of the physical processes under consideration. The similarity criteria under consideration are given in **Table 3.**

Table 3. Similarity criteria under consideration.

Criterion	Formula	Explanation
Reynolds number [15]	$Re = \frac{v \cdot d}{\nu}$, where $\nu$is the coefficient of kinematic viscosity, м^2 /s; v – speed, m/s; d– characteristic size, m.	The gas is subject to the forces of viscosity, pressure and inertia. Re is a value proportional to the ratio of viscous forces to inertial forces.

Criterion	Formula	Explanation
Euler's number	$Eu = \frac{\Delta p}{\rho \cdot v^2}$, where $\Delta p$is the pressure difference, Pa; ρ– density, kg/$м^3$.	A typical case is when the gas is affected by the forces of pressure and inertia Eu is a value proportional to the ratio of pressure forces to inertial forces.
Prandtl number	$Pr = \frac{\nu \cdot \rho \cdot c_p}{k}$, where $c_p$is the specific heat capacity, J /(kg · K), k– thermal conductivity coefficient, W /(m · K).	The Prandtl number is considered as a measure of similarity of temperature and velocity fields.
Boltzmann number	$Bo = \frac{\nu \cdot \rho \cdot c_p}{\sigma \cdot T^3}$, where $T$is the temperature, K; σ– Stefan-Boltzmann constant, $\sigma = 5{,}67 \cdot 10^{-8W}$ / (m2 · K ^{4}).	The Boltzmann number is the ratio of the intensity of convective heat transfer to the intensity of radiative heat transfer.
Schmidt number	$Sc = \frac{\nu}{D}$, where $D$is the diffusion coefficient, $м^2$/s.	Characterizes the relative role of molecular processes of momentum transfer and impurity mass transfer by diffusion The value of Sc shows how much more efficiently the impulse is transferred than the substance
Damköhler number	$Da_I = \frac{d \cdot W}{v \cdot \rho \cdot Y}$, where W is the reaction rate, kg $^/$(m3 · s); Y– concentration of the reactant.	Characterizes the ratio of the reaction rate to the rate of convective mass transfer.
The third number of Damkeller	$Da_{III} = \frac{Y \cdot d \cdot \Delta H \cdot k}{T \cdot v \cdot \rho \cdot c_p}$, where $\Delta H$is the thermal effect of a chemical reaction, k is the equilibrium constant.	Characterizes the ratio of the thermal effect of chemical reactions to the convective transfer of energy.

Table 3. (*Continued*)

3. Result and discussion

Figure 5 shows a diagram of the basic laboratory setup, on the basis of which, after modernization, it is planned to form a stand for studying combustion processes during combustion of methane in a carbon dioxide and oxygen environment. As can be seen from **Figure 4**, the stand uses natural gas from the general network, which is mixed with atmospheric air in the burner and burns in the combustion chamber, after which the combustion products are discharged into the ventilation. In the combustion chamber, non-hermetic selections are arranged for placing temperature and concentration sensors. The diagram of the stand and the materials from which the combustion chamber is made (refractory brick and sheet steel) do not allow conducting studies at high excess pressure.

In addition, the natural gas consumption in this stand is limited to 1.5 m3 $^/$ h, which corresponds to a thermal power of 15 kW, while the combustion chamber of the stand has a hydraulic diameter of 130 mm, which must be taken into account when planning experimental studies. To conduct tests, it is also necessary to develop a system for supplying pure oxygen and carbon dioxide, which act as an oxidizer and diluent, respectively.

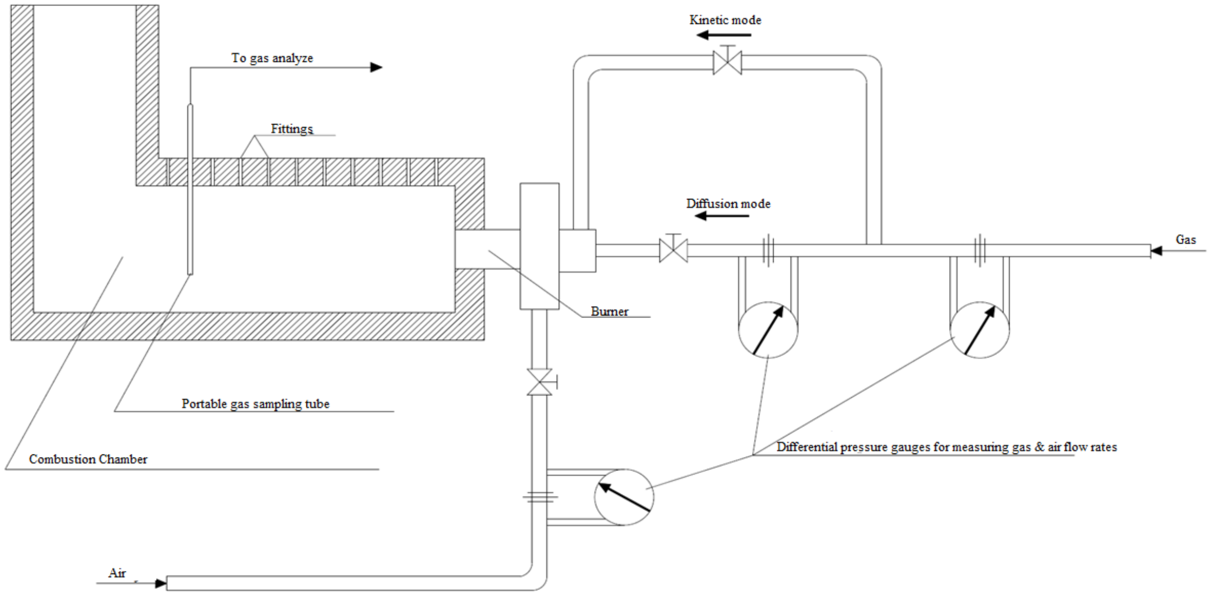

Figure 5. Laboratory setup diagram.

To ensure similarity of combustion processes in natural and model conditions, it is necessary to ensure equality of hydraulic diameters, flow rates and viscosity of the media. Equality of hydraulic diameters is ensured by the geometry of burner devices, and equality of flow rates is ensured by fixed power, which limits the power of a natural burner to 15 kW. In addition, in a natural burner device, the combustion process is carried out at the parameters of the Allam cycle, i.e. at high pressures and at temperatures of the working medium after compression and heating in the recuperator.

In this regard, it is necessary to take into account the difference in thermophysical properties, as well as the influence of temperature and pressure on the main similarity criteria in order to select the combustion mode of the experimental model burner device that would correspond to natural conditions. It is important to note that under the experimental conditions it is difficult to ensure heating of the fuel, oxidizer and diluent to temperatures corresponding to the Allam cycle, due to which the temperature of the media at the inlet was taken to be 293 K.

Since the main combustion processes occur at the fuel combustion temperature, it is necessary to estimate the combustion temperature for natural and model conditions. The theoretical (adiabatic) combustion temperature, calculated iteratively by the heat balance, was chosen as such a reference temperature. The main parameters of the model and natural burner devices are given in **Table 4**.

Table 4. Comparison of natural and model conditions.

Parameter	Experiment	Natural conditions
Hydraulic diameter, m	0.13	0.13
Heat of combustion of methane, J/kg	37500000	37500000
Power, W	15000	15000
Pressure, Pa	100000	30000000
Temperature of gases at the inlet, K	293	895
Estimated temperature for heat capacity, K	1449	1987,37

Table 5 shows the main parameters of the medium under model conditions, and **Table 4** – under natural conditions. The thermophysical properties of the gas mixture were taken after fuel combustion, and they were

calculated based on the properties of the mixture components using the additive method. As can be seen from **Tables 3** and **4**, due to the significant difference in temperatures (1450 K versus 1990 K) and pressures (30 MPa versus 0.1 MPa), the viscosity (by 20%), density (by 20 times) and thermal conductivity (by 3 times) of the media under model and natural conditions differ significantly. This fact requires adjustment of the burner device test modes in order to achieve similarity with natural conditions.

Table 5. Environmental parameters under model conditions.

Parameter	**CO2**	**CH4**	**O2**	**H2O**	**Total mixture**
Pressure, Pa	100000	100000	100000	100000	100000
Density, kg/ ^{m3}	0.37	0.13	0.27	0.15	0.34
Dynamic viscosity, Pa · s	$5.25 \cdot 10^{-5}$	$3.64 \cdot 10^{-5}$	$6.25 \cdot 10^{-5}$	$5.41 \cdot 10^{-5}$	$5.31 \cdot 10^{-5}$
Diffusion coefficient, m2/ s	4.72	4.72	4.72	4.72	0
Thermal conductivity, W/ (m · K)	0.10	0.28	0.10	0.16	0.11
Heat capacity, J/(kg · K)	1319.95	5467,13	1138,48	2584.94	1445.11
Mass fraction input	0.77	0.04	0.19	0,00	1.00
Mass fraction combustion	0.891	0	0,00891	0,1	1
Input flow rate, kg/s	0.0069	0,0004	0.00168	0	0.00898
Consumption after combustion, kg/s	0,008	0	0,00008	0,0009	0.00898

Table 6. Environmental parameters in natural conditions.

Parameter	**CO2**	**CH4**	**O2**	**H2O**	**TOTAL mixture**
Inlet temperature, K	939.05	655.55	387.65	0	895.4
Enthalpy at the entrance, J/kg	1176406,26	1887766,74	281.04	0,00	988060,36
Density, kg/ ^{m3}	75.28	27.34	55.40	32,32	70,80
Dynamic viscosity, Pa · s	$6.55 \cdot 10^{-5}$	$4.60 \cdot 10^{-5}$	$7.83 \cdot 10^{-5}$	$7.21 \cdot 10^{-5}$	$6.62 \cdot 10^{-5}$
Diffusion coefficient, m2 / s	0.0253	0.0253	0.0253	0.0253	0,00
Thermal conductivity, W/ (m · K)	0.33	0.39	0.12	0.27	0.33
Heat capacity, J/(kg · K)	1380.98	6137.35	1184.22	2883.24	1529,79
Mass fraction input	0.77	0.04	0.19	0,00	1.00
Mass fraction combustion	0.89	0,00	0.01	0.10	1.00
Input flow rate, kg/s	0.0069	0,0004	0.00168	0	0.00898
Consumption after combustion, kg/s	0,008	0	0,00008	0,0009	0.00898

Table 7 shows the similarity criteria data for the model and full-scale burner devices under basic conditions. As can be seen from **Table 5**, the similarity numbers differ significantly, both upwards and downwards, with the exception of the Schmidt number. The Prandtl number under full-scale conditions is 2.3 times smaller than under model conditions, the Reynolds number is 26% smaller, the Euler number is 20% larger, the Boltzmann number is 2.4 times smaller, the first Damkohler number is 9.5 times larger, and the third Damkohler number is 6.6 times larger. This is due to the fact that, at a fixed flow rate and hydraulic diameter, an increase in temperature leads to an increase in viscosity, which reduces the Reynolds number. On the other hand, an increase in temperature leads to an increase in the Damkohler numbers, which differ by an order of magnitude. Thus, it is impossible to simultaneously achieve similarity for all quantities, but it is possible to obtain similarity for individual processes, which requires an analysis of the influence of experimental parameters, in particular, pressure and thermal power on the similarity criteria.

Table 7. Comparison of natural and model conditions for current velocities and similarity criteria.

Parameters and criteria of similarity	Experiment	Natural conditions	Experimental/natural conditions ratio
Current speed, m/s	1.55	0.0075	206.67
Hydrodynamic similarity criteria			
Re	1300,08	1043	1.25
Eu	0.033	0.04	0.83
Similarity criteria for heat exchange processes			
Pr	0.72	0.31	2.32
Yes $_{III}$	47726,5	313043,1	0.15
Bo	4.45	1.83	2.43
Similarity criteria for mass transfer processes			
Sc	0.33	0.37	0.89
Yes $_{I}$	2093,66	19941,91	0.10

To assess this effect, various combinations of the model burner device power from 1.5 to 15 kW and pressures from 0.1 to 100 MPa were considered, and the ratios of similarity criteria were calculated as a percentage, i.e. 100% is a complete match. First of all, hydro gas dynamic similarity was considered. **Figures 6** and **7** show the dependences of the Reynolds and Euler numbers on the thermal power and pressure. As can be seen from **Figure 6**, with an increase in power, the Reynolds number grows, but the Euler number decreases. In this case, the pressure in the model burner device practically does not affect the ratio of the similarity criteria, which allows conducting hydrodynamic tests at atmospheric pressure. A compromise in terms of the Reynolds and Euler numbers is a configuration with a thermal power of about 12.5 kW, which ensures a model Reynolds number at the level of 103% of the natural one, and the Euler number at the level of 96% of the natural one, which is a good match. Thus, under model conditions, a good level of hydrodynamic similarity is achievable at a power of 12.5 kW, atmospheric pressure and a temperature of methane, oxygen and carbon dioxide of about 300 K at the inlet.

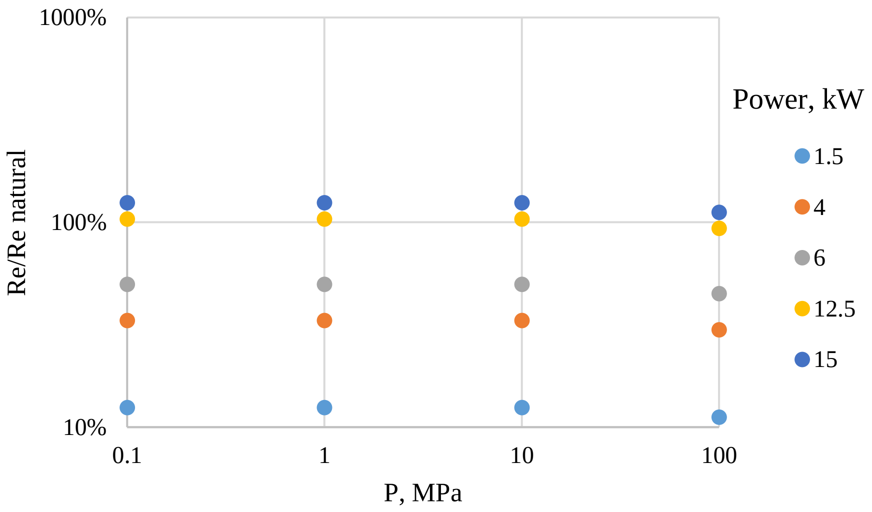

Figure 6. Dependence of the ratio of the model Reynolds number to the natural one on the power of the model burner device and pressure.

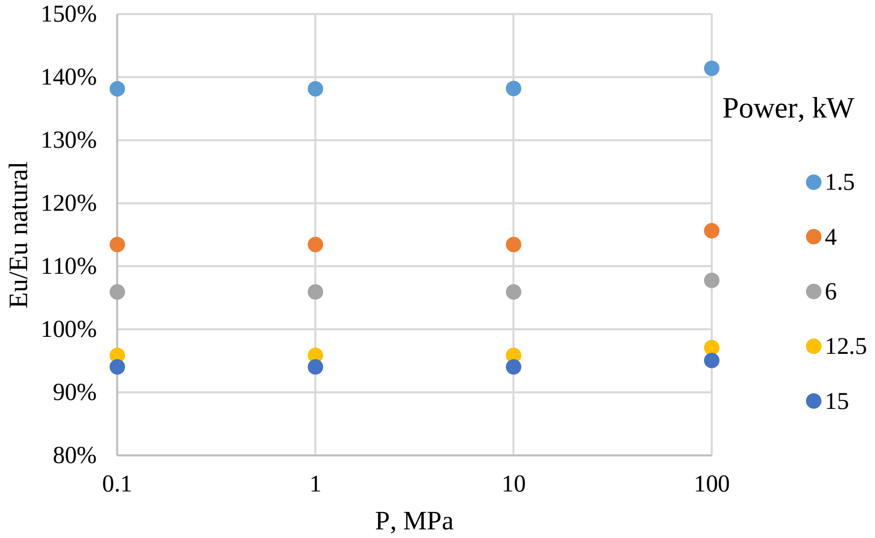

Figure 7. Dependence of the ratio of the model Euler number to the natural one on the power of the model burner device and pressure.

Thermal similarity criteria were also considered. **Figures 8**, **9**, **10** show the graphs of the Boltzmann, Prandtl and Damkohler (third) numbers versus power and pressure. As can be seen from the figures, the Boltzmann number increases with increasing power and weakly depends on pressure, the third Damkohler number decreases with increasing power, and the Prandtl number does not depend on power but depends on pressure. Under these conditions, complete thermal similarity for all criteria simultaneously is impossible. A compromise option is testing at a power of about 4 kW - in this case, the model Boltzmann number is ensured at 65%, the third Damkohler number at 60%, the Reynolds number at 33%, and the Prandtl number at 230%, which will ensure the Peclet number at 76% of the natural one. Thus, in this case, similarity is ensured according to the main criteria of similarity of heat exchange processes at a level of 60-70%, which is an acceptable level, but hydrodynamic similarity will not be ensured.

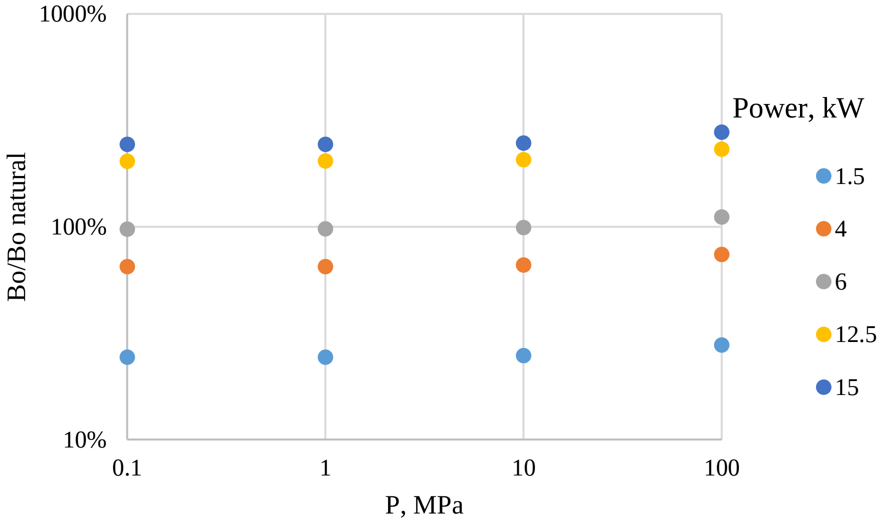

Figure 8. Dependence of the ratio of the model Boltzmann number to the natural one on the power of the model burner device and pressure.

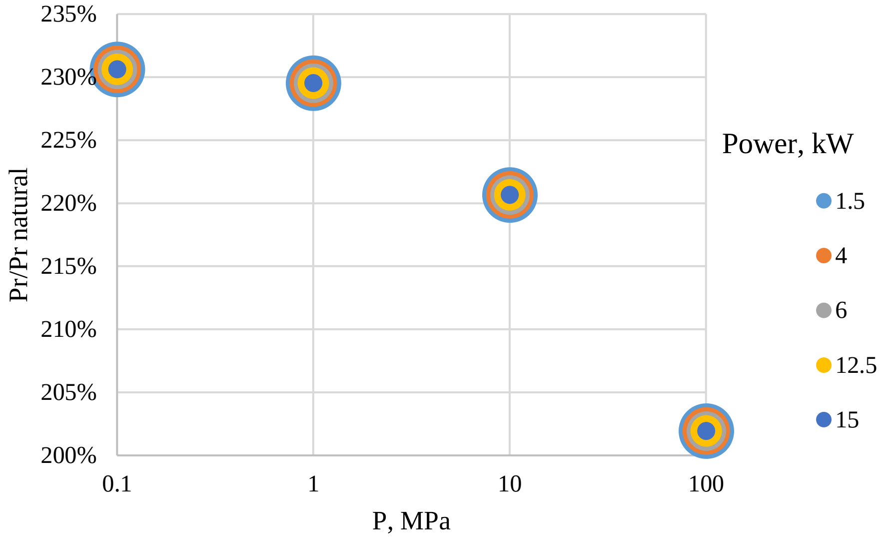

Figure 9. Dependence of the ratio of the model Prandtl number to the natural one on the power of the model burner device and pressure.

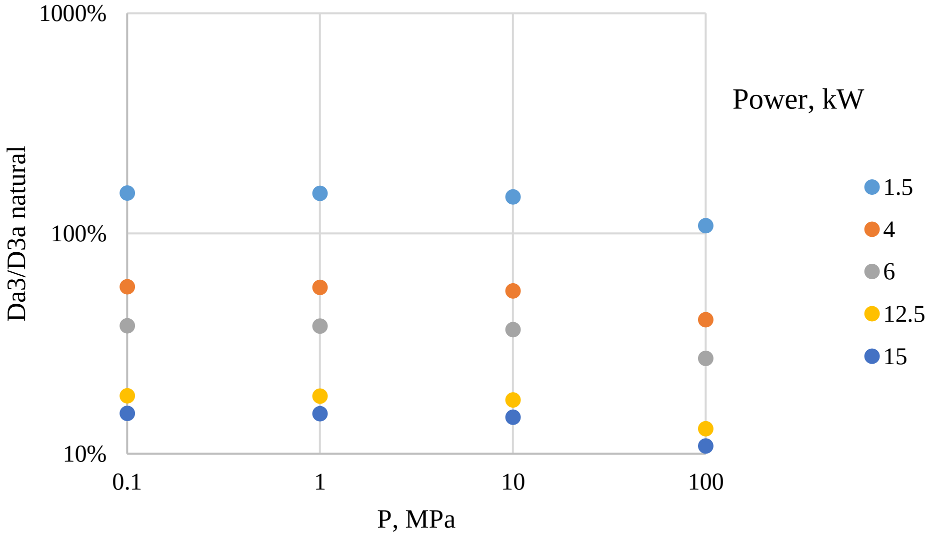

Figure 10. Dependence of the ratio of the model third Damköhler number to the natural one on the power of the model burner device and pressure.

The similarity was estimated in a similar manner from the point of view of mass transfer. **Figures 11** and **12** show the dependences of the Schmidt numbers and the first Damkohler number on the power and pressure during the tests. As can be seen from the figures, the Schmidt number is insensitive to the thermal power of the burner device, but changes with increasing pressure, while at atmospheric pressure it is at a level of approximately 90% of the natural one, which is a good approximation. However, to comply with the Sherwood criterion, a match in Reynolds numbers is also necessary, which is achieved at a power of 12.5 kW, but under such conditions the first Damkohler number is only 10% of the natural one, which is an unacceptably large difference. An intermediate power value of 4 kW in this case will provide both similarity criteria at a level of 30-40%, which is also a rough difference.

In this regard, it is more rational to conduct two tests to evaluate mass transfer processes: at a power of 12.5 kW to achieve similarity in terms of the Sherwood number and at a power of 1.5 kW to achieve similarity in terms of the first Damkohler number.

Thus, based on the analysis results, the burner device capacities were identified at which the required similarity criteria are achieved at atmospheric pressure and an input combustion component temperature of

293 K. To ensure hydrodynamic similarity, the model burner device capacity is required to be 12.5 kW, to ensure thermal similarity – 4 kW, to ensure similarity according to the first Damkler number – 4 kW, and according to the Sherwood number – 12.5 kW.

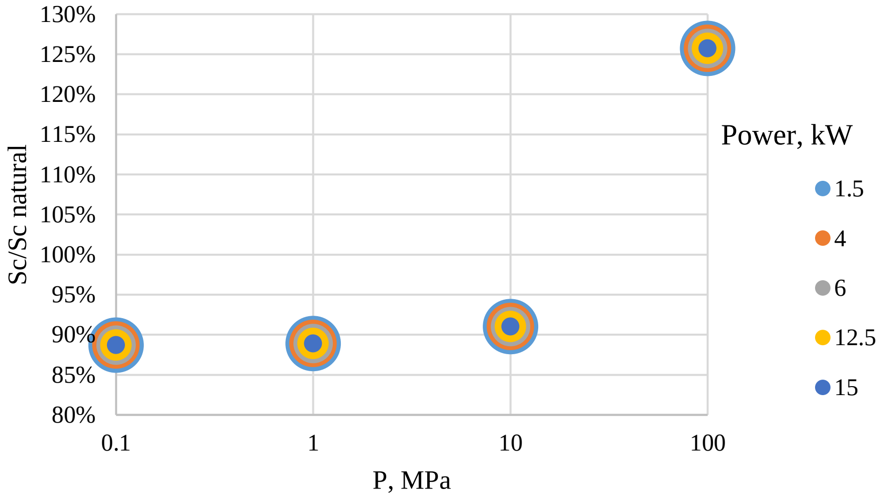

Figure 11. Dependence of the ratio of the model Schmidt number to the natural one on the power of the model burner device and pressure.

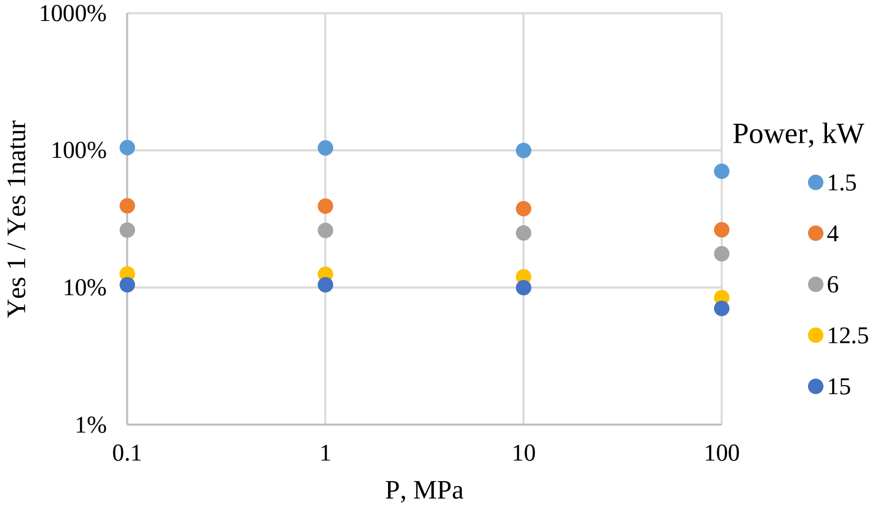

Figure 12. Dependence of the ratio of the model first Damköhler number to the natural one on the power of the model burner device and pressure.

From the point of view of the similarity of heat and mass transfer processes, the ratio of the conductive flow of thermal energy to the diffusion flow of mass, expressed by the Lewis number (Le), is also important. The Lewis number, by definition, can also be expressed as the ratio of the Schmidt number to the Prandtl number. As can be seen from **Figure 13**, in the pressure range of 0.1-10 MPa, the model Lewis number is at the level of 38-41% and approaches the natural one only at pressures above 100 MPa, and does not depend on the power of the burner device. However, with regard to the conditions under consideration with a clear predominance of convective components of mass and momentum transfer, a change in the ratio of molecular mass and energy flows within an order of magnitude will not have a significant effect.

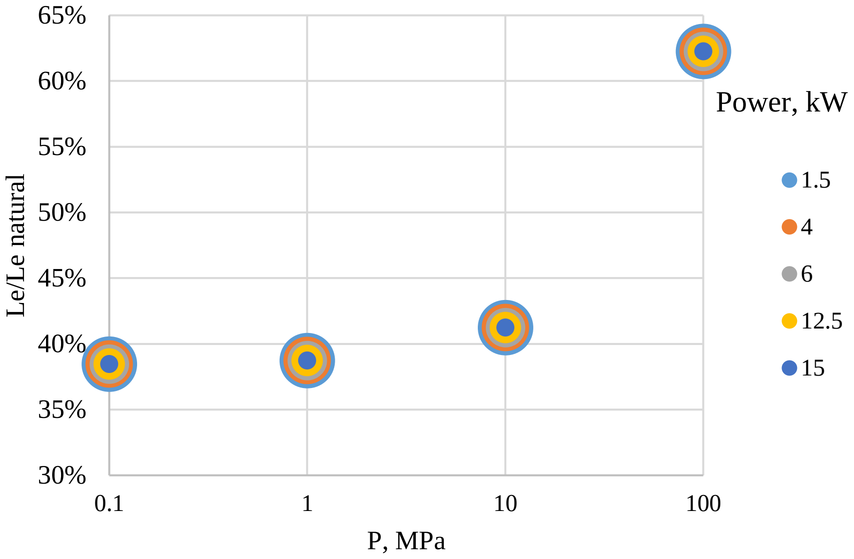

Figure 13. Dependence of the ratio of the model Lewis number to the natural one on the power of the model burner device and pressure.

4. Conclusion

The comprehensive analysis of the combustion processes of methane in an oxygen and carbon dioxide environment has yielded significant insights into the design and operation of burner devices for oxygen-fuel energy complexes (OFC). The study emphasizes the critical importance of achieving similarity between model and natural conditions to ensure the validity of experimental results and the applicability of findings to real-world scenarios.

1) The values of similarity criteria characterizing the processes of methane combustion in a mixture of carbon dioxide and oxygen, achievable in an experimental tunnel stand, providing testing of burner devices with a capacity of up to 15 kW, have been established: Reynolds number Re = 1300, Boltzmann number Bo = 4.5, the third and first Damköhler numbers Da III = 48000, Da I = 2100.

2) It has been determined that it is possible to reduce the deviation of the criteria for similarity of physical processes between a laboratory and a full-scale burner device of an oxygen-fuel combustion chamber only in the case of comparable thermal powers and equality of characteristic linear dimensions.

3) It has been established that the gas-dynamic processes occurring during atmospheric oxygen-fuel combustion will be similar to the gas-dynamic processes (in terms of Reynolds and Euler numbers) occurring in a full-scale oxygen-fuel combustion chamber with a power of 15 kW, with the power of the model burner device sample equal to 12.5 kW. With a 20% lower power of the model burner device relative to the full-scale one, the similarity of mass-exchange processes in terms of the Sherwood number will also be ensured. In order to ensure similarity in terms of heat exchange processes (Prandtl, Boltzmann numbers, the third Damkeller number) and mass-exchange processes in terms of the first Damkeller number during the experimental study of oxygen-fuel combustion, it is necessary to conduct tests at a power of the model burner device sample equal to 4 kW.

4) Taking into account the necessary operating parameters of the burner device to achieve similarity between the natural and laboratory processes of combustion of natural gas during oxidation with pure oxygen in a carbon dioxide environment, a scheme for upgrading the existing tunnel stand was developed, and a list of components for its modernization was determined.

Acknowledgments

This study conducted by National Research University "Moscow Power Engineering Institute" was supported by the Russian Science Foundation under Agreement No. 23-79-10291, https://rscf.ru/project/23-79-10291/

Author's Contribution

All Author contributed equally.

Conflict of interest

The authors declare that they have no conflict of interest.

About the author

Muhammad Maaz Shaikh: https://orcid.org/0009-0001-6142-2392

Sergey Osipov: https://orcid.org/0000-0002-5883-840X

References

1. Chan W. et al. Thermodynamic analysis and optimization of Allam cycle with a reheating configuration //Energy Conversion and Management. – 2020. – T. 224. – C.113382.
2. Zuev K. I. Fundamentals of similarity theory: lecture notes. – 2011, p.51.
3. Guryanov, A.I., Evdokimov, O.A., Guryanova, M.M. and Veretennikov, S.V. (2020). Criterion analysis and experimental study of combustion mechanisms in a bidirectional swirling flow and their relationship with pollutants emission. International Journal of Energy Research, 45(4), pp.5500–5516. doi:https://doi.org/10.1002/er.6178.
4. Norkin N. N. On approximate fire modeling of stationary gas combustion processes // Bulletin of Tomsk Polytechnic University. Engineering of Georesources. - 1948. - V. 64. - P. 220-231.
5. Anderson R. et al. Oxy-fuel turbo machinery development for energy intensive industrial applications //Energy Procedia. – 2014. – T. 63. – C. 511-523.
6. Saanum I., Ditaranto M. Experimental study of oxy-fuel combustion under gas turbine conditions //Energy & Fuels. – 2017. – T. 31. – №. 4. – C. 4445-4451.
7. Aminov R. Z., Schastlivtsev A. I. Experimental assessment of the composition of generated steam during combustion of hydrogen in oxygen // High Temperature Thermophysics. - 2020. - Vol. 58. - No. 3. - P. 437-444.
8. Roman Weber, Marco Mancini, On scaling and mathematical modelling of large scale industrial flames, Journal of the Energy Institute, Volume 93, Issue 1, 2020, Pages 43-51, ISSN 1743-9671, https://doi.org/10.1016/j.joei.2019.04.010.
9. Rene Prieler, Bernhard Mayr, Martin Demuth, Davor Spoljaric, Christoph Hochenauer, Application of the steady flamelet model on a lab-scale and an industrial furnace for different oxygen concentrations, Energy, Volume 91, 2015, Pages 451-464, ISSN 0360-5442, https://doi.org/10.1016/j.energy.2015.08.070.
10. Wang, S. and Shen, Y. (2025). CFD-DEM modelling of dense gas-solid reacting flow: Recent advances and challenges. Progress in Energy and Combustion Science, [online] 109, p.101221. doi:https://doi.org/10.1016/j.pecs.2025.101221.
11. Gratton, J. (1991). Similarity and Self Similarity in Fluid Dynamics.
12. Anders Rasmuson (2014). Mathematical modeling in chemical engineering. United Kingdom ; New York: Cambridge University Press, p.43.
13. Rapp, B.E. (2017). Chapter 9 - Fluids. [online] ScienceDirect. Available at: https://www.sciencedirect.com/science/article/abs/pii/B9781455731411500095.
14. Singh, M.R., Stevens, J.C. and Weber, A.Z. (2014). Design of Membrane-Encapsulated Wireless Photoelectrochemical Cells for Hydrogen Production. Journal of The Electrochemical Society, [online] 161(8), pp.E3283–E3296. doi:https://doi.org/10.1149/2.033408jes.
15. Saldana, M., Gallegos, S., Gálvez, E., Castillo, J., Eleazar Salinas-Rodríguez, Cerecedo-Sáenz, E., Hernández-Ávila, J., Navarra, A. and Toro, N. (2024). The Reynolds Number: A Journey from Its Origin to Modern Applications. Fluids, [online] 9(12), pp.299–299. doi:https://doi.org/10.3390/fluids9120299.